ARTICLE

Effect of Surfactant-Induced Modifications on CuCoMn Catalysts for Higher Alcohol Synthesis

Zhao-xia Zhang, Pei-yan Bi, Pei-wen Jiang, Quan-xin Li*

Department of Chemical Physics, Anhui Province Key Laboratory of Biomass Clean Energy, University of Science and Technology of China, Hefei 230026, China

(Dated: Received on April 28, 2014; Accepted on May 29, 2014)

A series of surfactant-modified CuCoMn-based catalysts were prepared for higher alcohol synthesis from biomass-based syngas. Three typical surfactants, cetyltrimethylammonium bromide (CTAB), sodium dodecyl sulfate (SDS) and pluronic P123 triblock copolymer ($EO_{20}PO_{70}EO_{20}$), were employed. Compared to surfactant-free CuCoMn catalyst, CO conversion increased from 17.4% to 29.7% over SDS-modified CuCoMn catalyst, and the selectivity of higher alcohols increased from 22.0% to 41.2% over CTAB-modified catalyst. Besides, the proportions of higher alcohols in total alcohols increased over all surfactant-modified catalysts. The catalysts were characterized by N_2 adsorption/desorption, XRD, XPS and IR analysis. The results showed that several more favorable features rendered the CTAB-modified CuCoMn catalyst to be suitable for higher alcohol production, such as the larger pore size, better crystallinity of $CuCoMnO_4$ spinel, moderate surface atomic distribution and lower valence of metallic ions. In addition, it was verified that CTAB addition at the metal precipitation stage was beneficial to higher alcohol synthesis. Surfactant-induced modification provides a promising alternative method for catalyst improvement in synthesis of higher alcohols.

Key words: Higher alcohol, Surfactant, Modification, CuCoMn catalyst

I. INTRODUCTION

Porous materials synthesized by a surfactant-templated process have attracted great interest in the past twenty years since the mesoporous M41S series were reported [1−4]. The surfactant-templated materials showed high surface areas and uniform pore sizes in the mesoporous range (diameter 2−50 nm), and the pore diameters could be tuned by adjusting the diameter of templating micelles. The formation mechanism of the ordered mesoporous structure was postulated the micellar arrays of surfactants template inorganic precursor with the subsequent and/or simultaneous condensation for cooperative assembly. The ordered mesoporous materials provide various potential applications in molecular recognition, such as shape-selective catalysis, which show high activities and product selectivities due to the high surface areas with more exposure of active sites on the surface and enhanced diffusion through the well-defined large mesopores [5−7]. Zou *et al.* reported the synthesis of mesoporous MnO_x-CeO_2 catalysts with high specific surface areas by using cetyltrimethylammonium bromide (CTAB) as templates, which was applied in the model reactions of CO and C_3H_8 oxidation [6]. Cao *et al.* also synthesized CuO-Fe_2O_3 and $CuO/Ce_{0.8}Zr_{0.2}O_2$ catalysts by using CTAB template [8, 9]. These catalysts displayed obvious advantages over those prepared by other methods, including high surface areas and wormhole-like mesoporous structures.

Higher alcohols (HA, $C_{2+}OH$), a mixture of C_2−C_6 alcohols, have wide applications such as alternative fuels, fuel additives and chemical raw materials [10−12]. Therefore, the catalytic conversion of syngas (CO and H_2) to HA has received renewed interest for both basic research and industrial application due to the abundant resources of syngas from coal, natural gas and biomass. Especially, biomass is an abundant and renewable resource which can contribute to a nonfossil-based feedstock for energy sources or chemicals [12]. Several heterogeneous catalysts for HA synthesis from syngas have been explored and well reviewed [13], including the modified methanol synthesis catalysts [14, 15], modified Fischer-Tropsch synthesis catalysts [16−21], noble metals-based synthesis catalysts [22], and Mo-based synthesis catalysts [23, 24]. Among them, CuCo-based modified Fischer-Tropsch catalysts developed by IFP (Institut Francais du Petrole) have been regarded as one of the most promising catalysts for HA synthesis owing to their relatively favorable reaction performance under mild operating conditions [25, 26]. These catalysts usually contained three or more metals from the group

*Author to whom correspondence should be addressed. E-mail: liqx@ustc.edu.cn, FAX: +86-551-63606689

Co, Cu, and Al, Mn, Zn, *etc.* and an alkali promoter (*e.g.*, La, K, Cs). They were generally prepared by co-precipitation method and the subsequent impregnation of alkali metal to obtain catalyst precursor with homogenous particles. The typical reaction conditions of HA synthesis for CuCo-based catalysts were 5−15 MPa, 490−620 K, 4000−8000 h^{-1} GHSV and a wide range of H_2/CO ratio. The reaction products of HA synthesis were mainly primary alcohols with relatively high selectivity of especially ethanol, depending on the type of the employed metal compositions. We have recently reported Na-promoted CuCoMn catalysts for conversion of bio-syngas to HA [27]. The results showed that the addition of sodium to the CuCoMn catalysts increased the selectivity of HA and promoted the dispersion of active elements (*i.e.*, Cu and Co). However, the rates of HA production (100−500 mg $C_{2+}OH/(g_{cat}$ h)) were obviously lower than those achieved in methanol synthesis (1300−1500 mg $MeOH/(g_{cat}$ h)) [13]. Thus, significant improvements in the HA synthesis must be further studied.

It is widely known that catalyst properties are greatly influenced by the preparation method. In this work, we tried to improve reaction performance of HA synthesis by surfactant-induced modification on CuCoMn-based catalysts. Three typical surfactants, namely cationic surfactant CTAB, anionic surfactant SDS (sodium dodecyl sulfate), and nonionic surfactant Pluronic P123 triblock copolymer ($EO_{20}PO_{70}EO_{20}$), were employed to investigate the different effects on the texture and surface chemical properties of CuCoMn oxides. The method of surfactant-induced modification provided a new approach for catalyst improvement in synthesis of higher alcohols.

II. EXPERIMENTS

A. Catalyst preparation

The chemicals used in this study were A. R. grade. The CuCoMn-based oxides were prepared with a settled molar composition: Cu/Co/Mn/Na=1/1/0.8/0.1. Three types of surfactants were employed: Pluronic P123 (Sigma-Aldrich), SDS, and CTAB (both from Sinopharm Chemical Reagent Company Limited, Shanghai, China). The surfactants were added into the CuCoMn precursors by two different strategies, named as co-pricipitation and post-precipitation methods. Detailed preparation procedure was as follows. A specific surfactant (P123, SDS, or CTAB) was predissolved in the sodium carbonate solution (so-called co-pricipitation method). Accordingly, the finally obtained CuCoMn catalysts were designated as CCM-P123, CCM-SDS, and CCM-CTAB respectively. Subsequently the mixture of metal nitrate solution (Cu, Co and Mn) was quickly added into the alkali solution at 343 K. The precipitate was kept in the mother liquor for 1 h, and then washed until the pH value of the final suspension was near 7.0. After being dried at 393 K for 12 h, the solid was impregnated with appropriate amount of Na_2CO_3, aged at 343 K for 2 h, and then calcined in air at 723 K for 4 h. The obtained CuCoMn oxide was further crushed and pelletized to tablets, and then sieved into 40−60 mesh particles for kinetic experiments. In addition, for comparison of the influence of different preparation method on CuCoMn catalyst, CTAB was introduced into inorganic precursors by physically mixing after metal precipitation and before calcination (so-called post-precipitation method, CCM-CTAB-PP). The catalyst without adding any surfactant was marked as CCM-NS.

B. Catalyst characterization

Powder X-ray diffraction (XRD) patterns were recorded on an X'pert Pro Philips diffractrometer (Philips, Netherlands), using a Cu Kα radiation (λ=0.15418 nm). The N_2 adsorption/desorption isotherms were measured at 77 K using the Micromeritics ASAP 2020 V3.00 analyzer. Pore size distributions and pore volumes were calculated using the Barrett-Joyner-Halenda (BJH) method on the desorption branch while BET (Brunauer-Emmett-Teller) surface areas were evaluated from the linear part of the BET plots. X-ray photoelectron spectroscopy (XPS) measurements were performed on an ESCALAB 250 (Thermo-VG Scientific, USA) spectrometer with Al Kα radiation. The C1s peak at a binding energy of 284.6 eV was generally fixed as a calibration standard for subtracting the surface charging effect. Infrared spectra (IR) of the samples were collected by a Bruker EQUINOX55 FTIR spectrometer, in the range of 400−4000 cm^{-1} at 0.5 cm^{-1} resolution. The specimens for measurements were prepared by mixing 3 mg of sample powder with 100 mg of KBr and then pressed into pellets.

C. Experimental setup and product analysis

The performance of HA synthesis from biomass-based syngas was evaluated in a fixed-bed continuous-flow reactor using an on-line gas chromatograph (GC) detection system [12, 27]. Generally, 1.0 g of catalyst diluted with 2.0 mL Pyrex beads was uniformly filled in the reactor (stainless steel 316 L, inner diameter: 10 mm, length: 400 mm). Before kinetic tests, the catalyst was reduced by a flowing 5vol%H_2/Ar at 593 K for 12 h. Then, the biomass-based syngas, including H_2, CO, CO_2, N_2, CH_4 and others with the volume contents of 62.80%, 30.89%, 2.96%, 1.75%, 1.20%, and 0.40% respectively [12, 27], was introduced into the reactor for HA synthesis under the designed conditions: T=553 K, P=5.0 MPa, and GHSV=4000 h^{-1} with dif-

DOI:10.1063/1674-0068/27/04/450-456

TABLE I Performance of HA synthesis over the CuCoMn-based catalysts modified by various surfactants. T=553 K, P=5.0 MPa, GHSV=4000 h^{-1}.

Catalyst	C_C/%	S_C/%			D/C-mol%						
		ROH	CO_2	C_xH_y	C_1	C_2	C_3	C_4	C_5	C_6	C_{2+}
CCM-NS	17.4	22.0	44.1	33.9	27.9	37.4	18.9	10.3	3.7	1.8	72.1
CCM-SDS	29.7	27.3	39.9	32.8	22.5	41.6	14.8	12.2	5.6	3.2	77.5
CCM-P123	23.5	16.7	47.5	35.8	22.9	40.3	16.1	14.3	4.3	2.1	77.1
CCM-CTAB	28.0	41.2	30.6	28.2	20.6	45.1	16.7	10.8	4.3	2.5	79.4
CCM-CTAB-PP	30.0	5.6	17.6	76.8	17.6	34.8	15.6	23.2	6.8	1.9	82.4

ferent CuCoMn catalysts. The gaseous products were analyzed on-line by GC (SP6890) with two detectors. H_2, CO, CH_4, and CO_2 were detected by a TCD detector with TDX-01 column, and gaseous hydrocarbons were determined by a FID detector with Porapak Q column. The organic condensates (mainly containing higher alcohols) cooled in a liquid tank were analyzed off-line by a FID detector. The performance of HA synthesis was evaluated by carbon conversion (C_C) of CO, carbon selectivity (S_C) of alcohols (ROH), CO_2 or hydrocarbon (C_xH_y), carbon yield (Y_C) of higher alcohols and alcohol distribution (D), according to the following equations:

$$C_C = \frac{a_{inCO} - a_{outCO}}{a_{inCO}} \times 100\% \quad (1)$$

$$S_C = \frac{b_1}{a_{inCO} - a_{outCO}} \times 100\% \quad (2)$$

$$Y_C = \frac{b_2}{a_{inCO}} \times 100\% \quad (3)$$

$$D = \frac{b_3}{x_C} \times 100\% \quad (4)$$

where a_{inCO}, a_{outCO}, and a_C are carbon moles of CO in, CO out, and carbon of all alcohols respectively, b_1, b_2, and b_3 are carbon moles in a certain product, higher alcohols, and C_xOH alcohol, respectively. The content of coke formed on the catalysts was negligent.

III. RESULTS AND DISCUSSION

A. Performance of HA synthesis

The performance of HA synthesis over CuCoMn-based catalysts modified by various surfactants was measured under the constant reaction conditions: 553 K, 5.0 MPa, and 4000 h^{-1}, the results are shown in Table I. Table I shows that all C_C increased when the surfactants (SDS, P123 and CTAB) were introduced into the CuCoMn catalysts. However, S_C of ROH followed different trends. The selectivities of alcohols over CCM-SDS and CCM-CTAB catalysts were enhanced to 27.3% and 41.2% respectively, while that over CCM-P123 catalyst decreased. Oppositely, the selectivities of

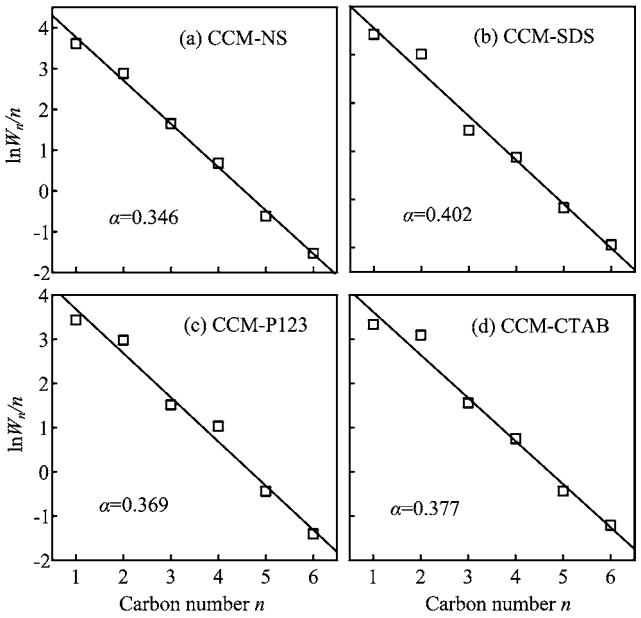

FIG. 1 ASF plots of alcohol products over CuCoMn-based catalysts modified by different surfactants. W_n, the mass fraction of an alcohol containing n carbon atoms.

CO_2 and hydrocarbon over the modified catalysts by surfactants decreased except P123, compared with the CCM-NS catalyst. In addition, Y_C of higher alcohols, increased from 2.8% on CCM-NS catalyst to 6.3%, 3.0% and 9.2% corresponding to CCM-SDS, CCM-P123 and CCM-CTAB catalysts respectively. CCM-CTAB catalyst showed the optimal yield of higher alcohols. Furthermore, in the alcohol distribution, Table I shows that the content of methanol decreased while that of higher alcohols ($C_{2+}OH$) presented an increasing trend by addition of surfactants into the CuCoMn-based catalysts. Especially, the amount of ethanol achieved more than 40% in the alcohol products. The results indicated that surfactant-induced modification on CuCoMn-based catalysts facilitates the formation of higher alcohols, and the catalyst added CTAB exhibits the highest HA selectivity, yield and distribution under the performed reaction conditions.

Figure 1 shows the ASF (Anderson-Schulz-Flory)

DOI:10.1063/1674-0068/27/04/450-456

TABLE II Textural parameters of CuCoMn-based catalysts modified by different surfactants. S_{BET}: Brunauer-Emmett-Teller surface area, V_p: pore volume, d_{XRD}: average crystallite size calculated by Sherrer equation.

Catalyst	$S_{BET}/(m^2/g)$	$V_p/(cm^3/g)$	d_{XRD}/nm
CCM-NS	75	0.23	6.25
CCM-SDS	58	0.21	6.03
CCM-P123	66	0.21	6.50
CCM-CTAB	15	0.16	6.80

plots for the alcohol distribution over surfactant-modified CuCoMn-based catalysts. Similar to the CuCoMn-based catalyst without adding surfactants [27], the alcohol products over the surfactant-modified CuCoMn-based catalysts followed excellent ASF ditributions except for a little deviation of ethanol from the ASF plots over CCM-SDS and CCM-CTAB catalysts. The chain growth probability (α) calculated from the slope of the ASF plot over the CCM-NS catalyst was 0.346, while those over surfactant-modified CuCoMn-based catalysts were between 0.369 and 0.402. The results indicated that adding surfactants into CuCoMn-based catalysts enhances the chain growth probability, which is consistent with alcohol distribution in Table I.

B. Characterization of catalysts

It is well known that the reaction performance of catalysts is closely related to their textural and surface chemical properties. The CuCoMn-based catalysts were characterized by N_2 adsorption/desorption, XRD, XPS and IR to investigate the enhancement of reaction performance by adding surfactants.

Table II lists the textural properties (BET surface areas S_{BET} and pore volume V_p) of CuCoMn-based catalysts added surfactants by co-precipitation methods. Interestingly, the S_{BET} of the surfactant-modified catalysts monotonously decreased in the following order: CCM-P123>CCM-SDS>CCM-CTAB. The order was just the opposite to those of alcohol selectivities (shown in Table I) and carbon yields. Also, the V_p followed similar trends with the minimum of 0.16 cm^3/g appearing in the CCM-CTAB catalyst. Generally, high surface areas favor more exposure of active sites on the surface consequently with high catalytic activities [6]. Even so, an exception [21] was reported that Co_3Cu_1 catalyst doped by activated carbon with 830 m^2/g of S_{BET} displayed lower conversion of CO and space-time-yields of (C_{1-8} alcohols+dimethyl ether), compared to the CNTs (h-type)-doped catalyst with 135 m^2/g of S_{BET}. The results indicated that surface area of catalyst is not the only determinant of the reaction performance.

The pore size distributions of the CuCoMn-based catalysts on the desorption branch calculated by BJH model are shown in Fig.2. The CCM-NS catalyst without adding surfactant had two pore sizes centred at 3.6 and 8.0 nm. The surfactant-modified CuCoMn-based catalysts (CCM-P123, CCM-SDS, and CCM-CTAB) possessed unique mesopores centered mainly at 8.8, 9.7, and 11.2 nm, respectively. From the resluts, it is concluded that the pore diameters of CuCoMn-based catalysts are enlarged and adjustable by adding surfactants. Moreover, the order of mesopore size distributions was in accordance with those of alcohol selectivities and carbon yields, which was attributed to enhanced molecular diffusions through the larger pores [5].

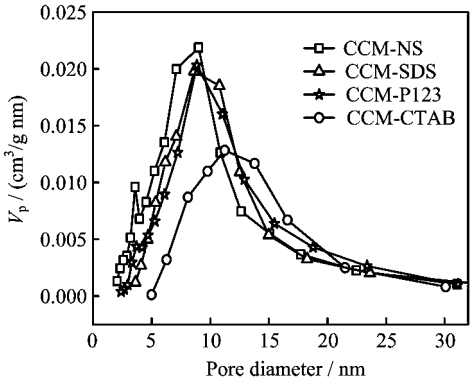

FIG. 2 The BJH pore size distributions on the desorption branch for CuCoMn-based catalysts modified by different surfactants.

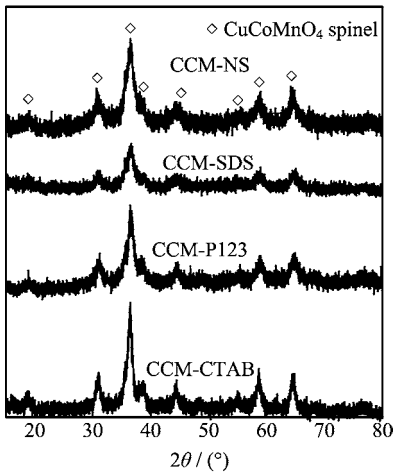

FIG. 3 XRD patterns of CuCoMn-based catalysts modified by different surfactants.

The XRD patterns of the CuCoMn-based catalysts by adding different surfactants are presented in Fig.3. All of the diffraction peaks in the figure can be attributed to spinel $CuCoMnO_4$ (JCPDS 47-0324). With addition of surfactants, the crystalline phases of CuCoMn-based catalysts were unchanged. However, the intensity of $CuCoMnO_4$ diffraction peaks changed. The XRD line width for CCM-SDS catalyst was broader than that for CCM-NS catalyst. In contrast, the diffraction peaks of

DOI:10.1063/1674-0068/27/04/450-456

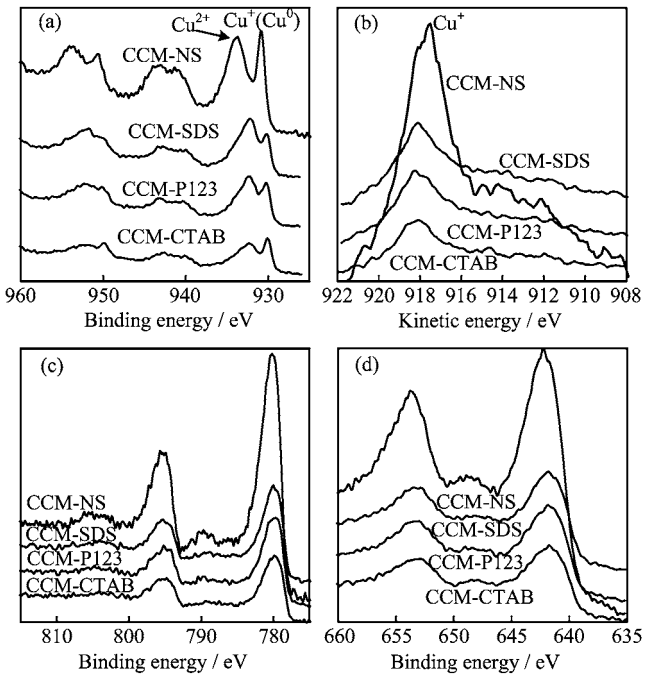

FIG. 4 XPS spectra of catalysts modified by different surfactants. (a) $Cu2p_{3/2}$, (b) Cu LMM, (c) $Co2p_{3/2}$, and (d) $Mn2p_{3/2}$.

$CuCoMnO_4$ for CCM-P123 and CCM-CTAB catalysts presented an increasing trend. The average crystallite sizes d_{XRD} calculated by XRD line widths of all peaks using Scherrer equation are listed in Table II. The crystallite size of $CuCoMnO_4$ in CCM-CTAB catalyst was the largest, which was consistent with its strongest intensity of diffraction peaks. $CuCoMnO_4$ spinel has been reported to be beneficial to stabilizing the active species of Cu^+ [28]. In addition, the increase of $CuCoMnO_4$ crystallite size in the CCM-CTAB was an indirect evidence for the remarkablely low specific surface area of 15 m^2/g revealed by N_2 adsorption/desorption results.

XPS is a surface analysis technique that can provide chemical state and surface elemental composition of the samples. The binding energies of the detected elements (Cu, Co and Mn) were calibrated at 284.6 eV with the C1s peak.

The $Cu2p_{3/2}$ XPS spectra of CuCoMn-based catalysts are shown in Fig.4(a). The binding energies at 930.8 and 933.9 eV in the CCM-NS catalyst without adding surfactant were observed, while those at 930.1±0.1 and 932.2±0.1 eV in the surfactant-modified catalysts were discovered. On copper oxides, the $2p_{3/2}$ peak of Cu^+ (Cu_2O) is at 932.2±0.3 eV and that of Cu^{2+} (CuO) is at 933.5±0.3 eV [28]. The sharp $Cu2p_{3/2}$ peak at 930.8 eV in Mn-containing CuCoMn oxides (CCM-NS) could be attributed to either Cu^+ or Cu^0. The $Cu2p_{3/2}$ peak at 933.9 eV in CCM-NS catalyst corresponding to Cu^{2+} was just at the right position. The fact represented that Mn induces the shift of Cu^+ (Cu^0) peak to lower binding energy. In addition, in the surfactant-modified catalysts (CCM-SDS, CCM-P123, and CCM-CTAB), the binding energies corresponding to Cu^{2+} (932.2±0.1 eV) in the $Cu2p_{3/2}$ spectra shifted as well as those corresponding to Cu^+/Cu^0 (930.1±0.1 eV). This negative chemical shift implies the changes of microchemical environment of Cu^{2+} due to the presence of surfactants.

Furthermore, the differentiation of Cu^+ and Cu^0 species could be achieved by combining with the Cu LMM Auger electron spectra (Fig.4(b)) [29, 30]. The Cu LMM spectra exhibited kinetic energies at 917.6, 918.1, 918.3, and 918.1 eV corresponding to the catalysts of CCM-NS, CCM-SDS, CCM-P123, and CCM-CTAB respectively. Modified Auger parameter α' is proposed to distinguish Cu^+ and Cu^0. This parameter, independent of the charging effect, is the sum of Cu^+/Cu^0 binding energy of the photoelectron line and the kinetic energy of the Auger line. All values of α' calculated from Fig.4 (a) and (b) were between 1848−1849 eV, which corresponds to Cu^+ rather than Cu^0 (1851−1852 eV) [29]. Additional evidence is that Cu^+ has a broad LMM Auger peak with its FWHM (full width at half maximum) over 2 eV, while Cu^0 has a very sharp LMM Auger peak with its FWHM about 1 eV [28]. In Fig.4(b), the Cu LMM Auger peaks of all catalysts were broad with their FWHM over 2 eV, thus indicating the presence of Cu^+ but not Cu^0. Therefore, the $Cu2p_{3/2}$ spectra of all fresh CuCoMn-based catalysts exhibited copper mainly as Cu^{2+} and Cu^+. It is worth noting that the presence of Cu^+ in the unreduced catalysts suggests the internal redox reaction of Cu^{2+} by Mn^{3+} ($Cu^{2+}+Mn^{3+}\rightarrow Cu^+ + Mn^{4+}$).

A summary of copper relative contents estimated by Gaussian fitting of the $Cu2p_{3/2}$ profiles in Fig.4(a) is shown in Table III. For CCM-CTAB catalyst, higher Cu^+/Cu^{2+} ratio (0.40) was observed compared to the other catalysts. The result agrees with the weakest shake-up satellite peak (941.4 eV) of Cu^{2+} about 9 eV higher than the binding energy of Cu^{2+} in Fig.4(a). According to Yan *et al.* [25], the amount of surface Cu^+ sites was responsible for methanol production rate as Cu^+ sites were essential for CO adsorption. Therefore, the high Cu^+/Cu^{2+} ratio in the CTAB-modified CuCoMn catalyst is more favorable for the CO conversion shown in Table I and consequently high yield of higher alcohols.

XPS spectra of Co are shown in Fig.4(c). The primary peaks (780.0±0.2 eV) are attributed to Co^{3+} or Co^{2+} without Co^0 species. The differentiation of Co^{3+} and Co^{2+} species could be obtained with the satellite peaks of $Co2p_{3/2}$. In the CCM-NS catalyst, Co^{3+} is obviously observed by a weak satellite peak (789.6 eV) at about 10 eV higher than its main peak. However, the intensities of satellite peaks assigned to Co^{3+} decreased in the surfactant-modified catalysts, and those assigned to Co^{2+} at 787.5−785.5 eV comparatively increased especially in the CCM-CTAB. The presence of

DOI:10.1063/1674-0068/27/04/450-456

TABLE III Surface composition of catalysts from XPS test.

Catalysts	Percentage/%			$Cu2p_{3/2}$ concentration		
	Cu	Co	Mn	Cu^+	Cu^{2+}	Cu^+/Cu^{2+}
CCM-NS	8.85	9.16	12.70	0.23	0.77	0.30
CCM-SDS	9.42	8.48	11.44	0.12	0.88	0.14
CCM-P123	8.88	8.32	11.96	0.19	0.81	0.23
CCM-CTAB	6.11	6.41	9.53	0.28	0.72	0.40

Co^{2+} also suggests internal reduction of Co^{3+} by Mn^{3+} ($Co^{3+}+Mn^{3+}\rightarrow Co^{2+}+Mn^{4+}$).

Figure 4(d) shows $Mn2p_{3/2}$ XPS spectra of the CuCoMn-based catalysts. In general, the binding energy of Mn^{4+} in MnO_2 is at 642±0.2 eV and that of Mn^{3+} in Mn_2O_3 is at 641.3 eV [28]. From Fig.4(d), the $Mn2p_{3/2}$ peak of surfactant-free CCM-NS catalyst was at 642.2 eV which was the right position of Mn^{4+}. The $Mn2p_{3/2}$ peaks of CCM-SDS and CCM-P123 catalysts are both at 641.9 eV. This value was slightly lower than that of Mn^{4+}, but noticeably higher than that of Mn^{3+}. It suggests that the surface Mn is mainly as Mn^{4+} in CCM-SDS and CCM-P123 catalysts. Unlikely, the $Mn2p_{3/2}$ peak of CCM-CTAB catalyst was at 641.7 eV. This value was between those of Mn^{4+} and Mn^{3+}, implying the coexistence of Mn^{4+} and Mn^{3+}. It can be concluded that Mn^{3+} was more attracted to the surface on the CTAB-modified CuCoMn catalyst. Moreover, the enriched Mn^{4+} on the surface is in agreement with the internal reductions of Cu^{2+} and Co^{3+} as discussed above.

The surface atomic percentages are listed in Table III. Interestingly, the metallic contents of Cu, Co and Mn ions in CTAB-modified catalyst were significantly lower than those in the other catalysts. From XPS results discussed above, the addition of CTAB into CuCoMn-based catalyst is more favorable for lower metallic contents on the surface and lower valence metallic ions. This correlation may be related to the repulsive interaction of positive charge CTAB carries to the metallic ions.

The CTAB-modified CuCoMn-based catalyst was spectroscopically measured by infrared spectra since its significantly lower S_{BET} and V_p were observed by N_2 adsorption/desorption analysis. It was suspected of blocking the holes in the catalyst by adding CTAB. From Fig.5, pure CTAB showed the C−H stretching bands at 2914 and 2850 cm^{-1} which was assigned to the -CH_2- groups [31]. Surprisingly, the C−H stretching bands in the range of 2980−2850 cm^{-1} disappeared nearly completely in the uncalcinated CuCoMn precursor modified by CTAB. It seems that the CTAB-modified CuCoMn precursor contains little or no CTAB after washing. It is assumed that the CTAB-induced modification on CuCoMn catalyst mainly occurred during the metal precipitation stage. Further verification was conducted by comparison of catalytic activity to the CTAB-modified CuCoMn catalyst by post-precipitation method.

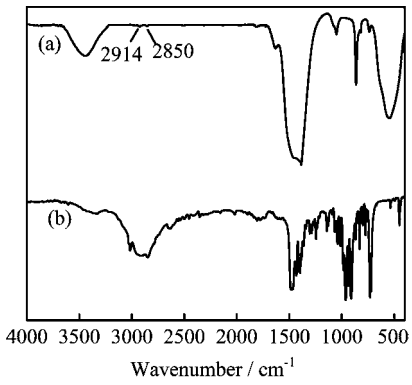

FIG. 5 IR spectra of (a) CCM-CTAB precursor before calcination and (b) pure CTAB.

C. Comparison between co-precipitation and post-precipitation on CTAB addition

A comparison was made with regard to the CTAB addition methods by CCM-CTAB and CCM-CTAB-PP, as shown in Table I. From Table I, the CO conversions of these two catalysts were in close proximity (28% and 30% respectively). The distinct differences in selectivities of alcohols and hydrocarbons were caused. The selectivity of alcohols over CCM-CTAB catalyst achieved 41.2% while that over CCM-CTAB-PP catalyst was just 5.6%. On the other hand, the selectivity of hydrocarbons over CCM-CTAB catalyst was 28.2% while that over CCM-CTAB-PP catalyst reached 76.8%. In addition, the hydrocarbon products (C_xH_y) obtained from CCM-CTAB catalyst were mainly composed of C_{1-4} gaseous hydrocarbons, while the content of C_{5+} liquid hydrocarbons in the total hydrocarbon products from CCM-CTAB-PP catalyst achieved 44.8C-mol%. These results indicated that different reaction pathways for CO hydrogenation probably occur on different active sites over the catalysts CCM-CTAB and CCM-CTAB-PP. Meanwhile, it can be taken as an important evidence that CTAB addition during metal precipitation stage is more favorable for higher alcohol synthesis over the modified CuCoMn catalyst.

IV. CONCLUSION

It was demonstrated that higher alcohols can be efficiently synthesized from biomass-based syngas using surfactant-modified CuCoMn-based catalysts. It was found that CO conversion increased from 17.4% on surfactant-free CuCoMn catalyst to 29.7% on SDS-modified CuCoMn catalyst prepared by co-precipitation method. Selectivity toward higher alcohols ($C_{2+}OH$)

DOI:10.1063/1674-0068/27/04/450-456

increased on the catalysts modified by SDS and CTAB. With respect to the alcohol products, the contents of higher alcohols in the total alcohols increased on surfactant-modified catalysts compared with that on surfactant-free catalyst. CTAB-modified CuCoMn catalyst showed the optimal catalytic performance. According to N_2 adsorption/desorption analysis, the pore diameters of surfactant-modified catalysts were enlarged and the pore diameter in CTAB-modified catalyst exhibited the largest in favor of molecular diffusions. XRD results suggested that $CuCoMnO_4$ spinel structure was the dominant phase for all fresh catalysts, which was favorable for stabilizing Cu^+ species. XPS analysis showed Cu, Co, and Mn mainly presented as Cu^+/Cu^{2+}, Co^{2+}/Co^{3+}, and Mn^{3+}/Mn^{4+} in the fresh catalysts, indicating the internal reductions of Cu^{2+} and Co^{3+} by Mn^{3+}. The CTAB-modified catalyst revealed lower metallic contents on the surface and lower valence metallic ions. Moreover, CTAB-induced modification during metal precipitation stage was confirmed to favor higher alcohol production. Present work reveals that surfactant modification is a promising method for catalyst improvement in synthesis of biomass-based higher alcohols.

V. ACKNOWLEDGMENTS

This work was supported by the National Key Basic Program of China (No.2013CB228105), and the National Natural Science Foundation of China (No.51161140331). The assistance of Song-bai Qiu and Tong-qi Ye from University of Science and Technology of China is gratefully acknowledged.

[1] L. Han and S. Che, Chem. Soc. Rev. **42**, 3740 (2013).
[2] M. Kruk, Accounts Chem. Res. **45**, 1678 (2012).
[3] C. T. Kresge, M. E. Leonowicz, W. J. Roth, J. C. Vartuli, and J. S. Beck, Nature **359**, 710 (1992).
[4] S. Cabrera, J. El Haskouri, J. Alamo, A. Beltrn, D. Beltrn, S. Mendioroz, M. D. Marcos, and P. Amors, Adv. Mater. **11**, 379 (1999).
[5] J. Kim, M. Choi, and R. Ryoo, J. Catal. **269**, 219 (2010).
[6] Z. Q. Zou, M. Meng, and Y. Q. Zha, J. Phys. Chem. C **114**, 468 (2010).
[7] J. Zhong, J. Li, F. Feng, S. Huang, and J. Zeng, Mater. Lett. **100**, 195 (2013).
[8] J. L. Cao, Y. Wang, T. Y. Zhang, S. H. Wu, and Z. Y. Yuan, Appl. Catal. B **78**, 120 (2008).
[9] J. L. Cao, Y. Wang, X. L. Yu, S. R. Wang, S. H. Wu, and Z. Y. Yuan, Appl. Catal. B **79**, 26 (2008).
[10] M. Ding, M. Qiu, J. Liu, Y. Li, T. Wang, L. Ma, and C. Wu, Fuel **109**, 21 (2013).
[11] J. J. Spivey and A. Egbebi, Chem. Soc. Rev. **36**, 1514 (2007).
[12] S. Qiu, W. Huang, Y. Xu, L. Liu, and Q. Li, Chin. J. Chem. Phys. **24**, 77 (2011).
[13] V. Subramani and S. K. Gangwal, Energ. Fuel **22**, 814 (2008).
[14] E. Heracleousa, E. T. Liakakoua, A. A. Lappas, and A. A. Lemonidou, Appl. Catal. A **455**, 145 (2013).
[15] R. G. Herman, Catal. Today **55**, 233 (2000).
[16] V. Mahdavi and M. H. Peyrovi, Catal. Commun. **7**, 542 (2006).
[17] N. Tien-Thao, M. H. Zahedi-Niaki, H. Alamdari, and S. Kaliaguine, J. Catal. **245**, 348 (2007).
[18] R. Xu, W. Wei, W. H. Li, T. D. Hu, and Y. H. Sun, J. Mol. Catal. A **234**, 75 (2005).
[19] R. Xu, C. Yang, W. Wei, W. H. Li, Y. H. Sun, and T. D. Hu, J. Mol. Catal. A **221**, 51 (2004).
[20] H. B. Zhang, X. L. Liang, X. Dong, H. Y. Li, and G. D. Lin, Catal. Surv. Asia **13**, 41 (2009).
[21] X. Dong, X. L. Liang, H. Y. Li, G. D. Lin, P. Zhang, and H. B. Zhang, Catal. Today **147**, 158 (2009).
[22] M. Ojeda, M. L. Granados, S. Rojas, P. Terreros, F. J. Garcia-Garcia, and J. L. G. Fierro, Appl. Catal. A **261**, 47 (2004).
[23] J. Iranmahboob, H. Toghiani, D. O. Hill, and F. Nadim, Fuel Process. Technol. **79**, 71 (2002).
[24] Z. Li, Y. Fu, J. Bao, M. Jiang, T. Hu, T. Liu, and Y. N. Xie, Appl. Catal. A **220**, 21 (2001).
[25] Q. Yan, P. T. Doan, T. Hossein, C. G. Amit, and G. W. Mark, J. Phys. Chem. C **112**, 11847 (2008).
[26] P. Mohanty, K. K. Pant, J. Parikh, and D. K. Sharma, Fuel Process. Technol. **92**, 600 (2011).
[27] T. Q. Ye, Z. X. Zhang, Y. Xu, S. Z. Yan, J. F. Zhu, Y. Liu, and Q. X. Li, Acta Phys. Chim. Sin. **27**, 1493 (2011).
[28] B. L. Yang, S. F. Chan, W. S. Chang, and Y. Z. Chen, J. Catal. **130**, 52 (991).
[29] G. Deroubaix and P. Marcus, Surf. Interface Anal. **18**, 39 (1992).
[30] S. Velu, K. Suzuki, and C. S. Gopinath, J. Phys. Chem. B **106**, 12737 (2002).
[31] Y. Mitsunori, H. Hiroaki, O. Kaoru, M. Masato, and K. Tsuyoshi, Inorg. Chem. **36**, 5565 (1997).

DOI:10.1063/1674-0068/27/04/450-456